ISSN 0915-6364

NATIONAL INSTITUTE FOR FUSION SCIENCE

Transitions between Fine-structure Levels of *FeXX* Ion in Collisions with Protons in High-temperature Plasmas

A.D. Ulantsev and I. Murakami

(Received - July 20, 2010)

NIFS-DATA-111 July 27, 2010

RESEARCH REPORT
NIFS-DATA Series

TOKI, JAPAN

Transitions between fine-structure levels of $FeXX$ ion in collisions with protons in high-temperature plasmas.

A. D. Ulantsev
Gubkin Russian State University of Oil and Gas, Moscow, Russia *

I. Murakami
National Institute for Fusion Science

July 20, 2010

Abstract

Proton-impact excitation cross sections and excitation rate cofficients for transitions among all the ground state fine-structure levels of Fe XX ion $1s^2 2s^2 2p^3$ $(S_{3/2}, D_{3/2}, D_{5/2}, P_{1/2}, P_{3/2})$ were computed. The close-coupling approximation of the impact-parametre method with the Coulomb trajectories of the relative motion of nuclei was used. All the m-components of the initial and final target states were taken into account. The interaction matrix elements between target states were calculated numerically for every step of integration with the wave functions of $2p^3$ electronic configuration written in the intermediate coupling scheme with the numerical semi-empirical one-electron functions (Shevelko and Vainstein 1993, it Atomic Physics for Hot Plasma) The excitation rate cofficients were calculated for the temperature range 3×10^6 - 6×10^8K and compared with the only available results of semiclassical approximation (first perturbative approximation of the impact parametre method) (Bhatia and Mason 1980, Astron. Astrophys. 83, 380) in the temperature range 6×10^6 - 1.5×10^7K. The calculated close coupling values of the excitation rate cofficients are found to be somewhat smaller than the semiclassical results (Bhatia and Mason 1980) in the temperature overlapping interval.

Keywords: atomic data, proton-impact excitation, Fe XX, close-coupling method

*The work was made during the visit of A. D. Ulantsev to NIFS.

1 Introduction

Since the pioneer work of Seaton [1] it is a common knowledge fact that collisions of ions, including multicharged ions, with protons may play important role for the energetic level populations, the radiation emission and the energetic balance in high temperature astrophysical (Solar corona and nebulae) and laboratory (themonuclear reactors) plasmas. In the case of multicharged ions at temperatures typical for Solar corona or laboratory plasmas the contribution of proton collisions may be comparable with the contribution of electron collisions mainly for transition between fine-structure levels. It is worth recalling that in beam-heated, magnetically confined plasmas, as in modern thermonuclear reactors, the ion temperature T_i, for example the proton temperature T_p, may be much larger than T_e [2]. That may substantially increase the role played by the proton-ion collisions even if the proton excitation rates are much less than the electronic excitation rates at *equal* temperatures.

Taking into account the huge technical difficulties of experiments with the multicharged ion beams that are necessary to measure the excitation cross sections, the role of reliable theoretical results is very important. For majority of Fe^{q+} ions there exist a number of the theoretical results obtained through methods of different complexity. The comparison of different results allows to choose the most reliable ones and to estimate their probable accuracy. The review of these works with the analysis of the accuracy of their results and convenient fit expressions for corresponding proton excitation rates was published recently [3, 4, 5].

Looking through the list of references of the review[3] it is easy to see that the ion $FeXX = Fe^{19+}$ is a kind of exception among other Fe ions. Only one set of computational results on proton excitation rates was published rather long ago for this ion [6]. These results were obtained in the well known semiclassical approximation for collisions with the inclusion of the Coulomb interaction of partners [7], that is in the first approximation of the perturbation theory in the frames of impact parametre method with the Coulomb trajectories of the nuclei of the partner ions and with quadrupole potential of interaction having a singularity at small internuclear distance. It is worth noting also that the information on the input data for computations was very scarce in the publication in question. In particular, only total probabilities for forbidden radiative transitions between fine-structure levels were given in [6]. These total transition probabilities equal the summs of E2 (electric quadrupole) and M1 (magnetic dipole) transition probabilities, yet for computation of the proton excitation cross sections and rates even with the simplest quadrupole potential it is necessary to know the quadrupole (E2) transition probabilities separately[1, 8]. So the parametres of the interaction potential used in [6] remain unclear. One may assume that the extreme scarcity of information on the proton excitation of $FeXX$ is connected with the difficulties of the detailed description of electronic states with the $2p^3$ configuration, though from the other side the situation with the proton excitation cross sections and rates for the $FeXII$ ion having the configuration $3p^3$ is much more satisfactory [4]. Anyway we found important to revisit the problem of the proton excitation of the ground state fine-structure levels of the $FeXX$ ions using more elaborate computation techniques than before and also to use more recent and reliable input data.

We computed the proton excitation cross sections for the energy interval 0.3-400 keV/amu and also the proton excitation rates for the temperature interval $3\times10^6 - 600\times 10^6$ K in the close-coupling approximation of the impact-parametre method. The target atomic basis consisted of the intermediate-coupling wave functions for the external shell with $2p^3$ configuration constructed from one-electron semi-empirical wave functions [9]. The system of ordinary differential equations for the amplitudes was solved numerically. The system describing the transitions from one of the M_J-components of the initial energy level took into account the close-coupling of the inital state with *all* the $M'_{J'}$-components of the final energy level (up to 6 final states). The matrix elements of the interaction potential taking into account the angular parts of the basis wave functions were calculated numerically during the solution of the system of ordinary differential equations. The Coulomb trajectory of the projectile proton corresponding to the constant modulus of the relative velocity (speed) was used[1]. The excitation cross sections for transitions between the fine-structure levels and corresponding excitation rates were obtained by summing over the final magnetic states and averaging over the initial magnetic states. The proton excitation cross rates are compared with the semiclassical approximation results [6]. The cross-sections for the transitions $^2D_{3/2} - ^2P_{3/2}$ and $^2D_{5/2} - ^2P_{1/2}$ are compared with the Born-Coulomb approximation results computed by ATOM program [9].

2 The scheme of computations

The absolute majority of results for the proton excitation of multicharged ions were obtained with the use of the impact parameter method providing for the classical trajectories of the nuclei of heavy partnes [8, 4, 3]. It concerns both perturbative methods and more refined approaches as close coupling of a number of states from some basis set. As it is well established in the literature, the impact parameter method is accurate enough already at energies above tens of electonvolts per nucleon. Correspondingly we use the impact parameter method for all the energies in question. As we ignore the necessarilly small probabilities of electron capture by the impinging proton, the electron wave function of the system in the frames of the impact parametre method may be presented as a linear combination of the wave functions describing the unperturbed states of the target ion with $N = 3$ "active" electrons[2]. Using the :

$$\Psi(\mathbf{r}_1,\xi_1,...\mathbf{r}_3,\xi_3;t) = \sum_{\alpha,J,M_J} a_{\alpha,J,M_J}(t)\varphi_{\alpha,J,M_J}(\mathbf{r}_1,\xi_1,...\mathbf{r}_3,\xi_3)e^{-iE_{\alpha,J}t}. \qquad (1)$$

where $\mathbf{r}_k$, ξ_k are the coordinate vector and the spin projection variable of the k-th electron, α-the totality of quantum numbers beside the total angular momentum number J and its projection number M_J. In the case in question the indexes α, J define the definite fine-structure energy level in the intermediate coupling approximation [16, 17] so $\alpha =^{2S+1} L'_J$, and in the approximation used in the work $\alpha, J =^4 S'_{3/2};^2 D'_{3/2};^2 D'_{5/2};^2 P'_{1/2};^2 P'_{3/2}$.

[1]It is worth noting that the method developed allows after the slight modificaton to take into account the variation of speed during collision due to static and dynamic screening of the target nucleus by the electron distribution and the corresponding deflexion of the "exact" classical trajectory of the projectile proton from the Coulomb hyperbola.

[2]Atomic units $e = m = \hbar = 1$ are used throughout the paper unless it is indicated otherwise.

Here the prime sign near the total orbital momentum quantum number recalls about the intermediate coupling approximation used. So the model takes into account 5 energy levels of the ground configuration of the ion. The total number of M_J components taken into account equals 20.

Substituting the expansion (1) into the time-dependent Schrödinger equation and projecting the resulting equation onto the the orthonormal set of the basis functions $\varphi_{\alpha,J,M_J}(\mathbf{r}_1,\xi_1,...\mathbf{r}_3,\xi_3)$, we obtain the system of close-coupling equations in the impact parametre approach, that is the system of first order ordinary differential equations for the amplitudes $a_{\alpha,J,M_J}(t)$:

$$i\dot{a}_{\alpha,J,M_J}(t) = \sum_{\tilde{\alpha},\tilde{J},\tilde{M}_J} V_{\alpha,J,M_J;\tilde{\alpha},\tilde{J},\tilde{M}_J}(\mathbf{R}(t)) a_{\tilde{\alpha},\tilde{J},\tilde{M}_J}(t) e^{-i(E_{\alpha,J}-E_{\tilde{\alpha},\tilde{J}})t} \tag{2}$$

where the function $\mathbf{R}(t)$ determines the trajectory of the projectile. The potential of interaction $V(\mathbf{r}_1,...\mathbf{r}_3;\mathbf{R}(t))$ has the form

$$V(\mathbf{r}_1,...\mathbf{r}_3;\mathbf{R}(t)) = -\sum_{k=1}^{3} \frac{Z_P}{|\mathbf{r}_k - \mathbf{R}(t)|} \tag{3}$$

where the projectile charge $Z_P = 1$ for the proton collisions that is our case . The expressions for the matrix elements

$$V_{\alpha,J,M_J;\tilde{\alpha},\tilde{J},\tilde{M}_J}(\mathbf{R}(t)) =< \varphi_{\alpha,J,M_J}(\mathbf{r}_1,\xi_1,...\mathbf{r}_3,\xi_3)|V(\mathbf{r}_1,...\mathbf{r}_3;\mathbf{R}(t))|\varphi_{\tilde{\alpha},\tilde{J},\tilde{M}_J}(\mathbf{r}_1,\xi_1,...\mathbf{r}_3,\xi_3) > \tag{4}$$

are given in Appendix A. The initial conditions for the system (2)

$$a_{\alpha,J,M_J}(t \to -\infty) = \delta_{\alpha,\hat{\alpha}}\delta_{J,\hat{J}}\delta_{M_J,\hat{M}_J} \tag{5}$$

where the indexes $\hat{\alpha},\hat{J},\hat{M}_J$ define the initial state. So the solutions $a_{\alpha,J,M_J}(t)$ depend implicitly on the initial state and are to be designated more presisely $a_{\alpha,J,M_J;\hat{\alpha},\hat{J},\hat{M}_J}(t)$, but the indexes of the initial state are omitted if not absolutely necessary. If the collision energy $E = m_p v_i^2/2$ considerably exceeds the maximum excitation energy

$$max(E_{\alpha,J} - E_{\alpha',J'}) << E \tag{6}$$

the trajectory $\mathbf{R(t)}$ may be chosen as the solution of the classical dynamics equation with the Coulomb potential of interaction between the projectile and the target

$$m_p\ddot{\mathbf{R}}(t) = \frac{Z_p Z_T \mathbf{R}(t)}{R^3(t)} = -\nabla(\frac{Z_P Z_T}{R(t)}) \tag{7}$$

where for the case in question $Z_P = 1$ and the target charge $Z_T = 19$. The strict initial conditions for the equation (7) have the form:

$$\mathbf{R}(t \to -\infty) = \mathbf{b} + \mathbf{v_i}t; \dot{\mathbf{R}}(t \to -\infty) = \mathbf{v_i} \tag{8}$$

where b is the impact parametre. During the numerical solution the conditions (8, 5) were naturally replaced by the similar conditions at large but finite internuclear distance

$R(t_0) = R_{max} = 50, \quad t_0 < 0$. As the recomputings with smaller values of R_{max} have shown, this choice guaranteed the independence of the computation results from the starting point.

It is worth recalling that strictly speaking the simple form of the classical dynamics equation (7) is valid only under additional condition

$$|\mathbf{R}|_{min} >< r > \tag{9}$$

where the minimal internuclear distance $|\mathbf{R}|_{min} = 2b^2E/(\sqrt{Z_P^2 Z_T^2 + 4E^2b^2} - Z_P Z_T), \quad b \neq 0$, and the average radial coordinate of an "active" electron $< r > \approx n^2/(Z_T + 1), \quad n = 2$. If some of the conditions of validity of the equation (7) is violated, the more general classical dynamics equation may be used, taking into account the distributed electron charge. One can use in this equation either the static distribution corresponding to the initial electronic state of the target or the dynamical electron distribution expressed by means of the time-dependent electronic wave function (1).

After the numerical solution of the close-coupling system of the differential equations the excitation probabilities for the M_J components are expressed in a standard way

$$p_{\hat{\alpha},\hat{J},\hat{M}_J \to \alpha,J,M_J}(v_i, b) = |a_{\alpha,J,M_J}(t \to \infty)|^2 \tag{10}$$

In practice the solution procedure was finished when the internuclear distance reached the value $R(t_m) = R_{max} = 50, \quad t_m > 0$. The cross section for transition from the state $\hat{\alpha}, \hat{J}\hat{M}_J$ to the state α, J, M_J are also expressed in a common way

$$\sigma_{\hat{\alpha},\hat{J},\hat{M}_J \to \alpha,J,M_J}(v_i) = 2\pi \int_0^\infty p_{\hat{\alpha},\hat{J},\hat{M}_J \to \alpha,J,M_J}(v_i, b) b db \tag{11}$$

In the numerical realisation the upper limit of the integration is replaced by $b_m = R_{max}/2$. After the computation of the cross sections for all the $\hat{M}_J$ components of the initial energy level $E(\hat{\alpha}, \hat{J}) = E(^{2\hat{S}+1}\hat{L}_{\hat{J}})$ the total cross section of the transition from the initial level to another energetic level $E(\alpha, J) = E(^{2S+1}L_J)$ may be obtained through summing over final components M_J and averaging over initial components $\hat{M}_J$, that is expressed as

$$\sigma_{\hat{\alpha},\hat{J} \to \alpha,J}(v_i) = \frac{1}{2\hat{J}+1} \sum_{\alpha,J,M_J} \sum_{\hat{\alpha},\hat{J},\hat{M}_J} \sigma_{\hat{\alpha},\hat{J},\hat{M}_J \to \alpha,J,M_J}(v_i) \tag{12}$$

The program for the numerical solution of the system (2, 7) with the initial conditions (5, 8) was written in the MATHCAD system (version MATHCAD-13). To check the correctness of the program functioning the computations were made for the transition probabilities between the fine structure levels of the B-like ion FeXXII. The cross sections for the transition $^2P_{1/2} - ^2P_{3/2}$ transition at the collision energies 0.8–50 keV/amu were compared with the results of [11] obtained also in the frames of the close coupling approximation with the Coulomb trajectory. In [11] the interaction potential for long internuclear distances was expressed in terms of the E2 transition strengths, and for short distances was corrected with the factor containing the approximate H-like wave functions of the corresponding state. Besides the configuration interaction was approximately taken into

account by the method of the polarization potential [12, 13]. Our results coincide with the results of [11] within 8% for the collision energies 0.8–3 keV/amu, that is below and near the cross section maximum, but go above the results of [11] with almost constant factor of 1.5. That may be connected with the differences in the interaction potentials and the effect of the polarization potential, but the functioning of the program seems quite correct.

3 The computation results.

3.1 The results for the total cross sections.

The total proton excitation cross sections for transitions between the fine-structure levels of the ground state of the $FeXX$ ion are presented in Tab. 1 and plotted in Figures 1, 2, 3. In Figures 2, 3 the plots of the computed total cross section for the transitions $^2D_{3/2} \rightarrow^2 P_{3/2}$ and $^2D_{5/2} \rightarrow^2 P_{1/2}$ may be compared with the plots of the corresponding Born-Coulomb cross sections computed with the ATOM program [9]. It is easy to see that the close coupling and Born-Coulomb curves are very close at energies above 10 keV/amu. The remaining descrepancies (30-40%) are partialy connected with the use of LS wave functions in the ATOM program and may be partially the result of the finite integration area in the equation (11). One can not also exclude the effect of the accumulation of the round-off errors that becomes more noticeable for small values of the cross sections.

Regretfully, we do not know publications on the cross sections for the proton excitation from the $^4S_{3/2}$ level, so we have no possibility to compare our results with any results of other authors.

3.2 The results for the rate constants.

The proton excitation rate constants are given in Tab. 2. The temperature dependencies of the rate constants are also presented in Figs. 4, 5, 6 in comparison with the results of Bhatia and Mason [6] calculated in semiclassical approximation.

It is seen that for the majority of the transitions the close coupling results for the excitation rates constants are lower than the semiclassical (the first perturbative approximation) resuls with a factor about two. Beside the effect of close coupling that in majority of cases diminishes the cross sections it is worth noting again the fact that in the work referenced [6] lacked the information on the separation of electric quadrupole (E2) and magnetic dipole (M1) contribution to the radiative spontaneous probabilities and the line strengths that were used for the estimation of the quadrupole interaction potential.

4 Conclusions.

We computed in the first time the cross sections and the rate constants for the proton excitation of the fine structure levels of the ground state configuration of the FeXX ion in the close coupling approximation of the impact parametre approach with the Coulomb trajectories of the nuclei for rather wide intervals of the collision energies and the proton

Table 1: The proton excitation total cross sections, $\sigma(10^{-19}$ cm$^2)$. Here $a \pm b \equiv a \times 10^{\pm b}$.

Energy (keV/amu)	0.3	0.6	1.2	2.4	4.8
$^4S_{3/2} - ^2D_{3/2}$	7.63-11	3.24-3	1.58	7.03	5.26
$^4S_{3/2} - ^2D_{5/2}$	3.03-11	6.95-4	2.19	1.78+1	1.62+1
$^4S_{3/2} - ^2P_{1/2}$	8.50-13	2.10-7	2.18-2	6.45-1	8.45-1
$^4S_{3/2} - ^2P_{3/2}$	3.11-13	1.82-9	2.76-4	2.18-2	3.69-2
$^2D_{3/2} - ^2D_{5/2}$	2.86-2	3.27	1.48+1	1.79+1	1.08+1
$^2D_{3/2} - ^2P_{1/2}$	1.76-8	6.94-2	1.05+1	3.11+1	2.18+1
$^2D_{3/2} - ^2P_{3/2}$	3.24-11	5.83-4	1.85	1.48+1	1.33+1
$^2D_{5/2} - ^2P_{1/2}$	9.19-6	0.2.39-1	7.42	1.66+1	1.19+1
$^2D_{5/2} - ^2P_{3/2}$	4.22-10	2.66-2	11.3	4.01+1	2.50+1
$^2P_{1/2} - ^2P_{3/2}$	8.34-4	1.39	1.46+1	2.09+1	1.25+1

Energy (keV/amu)	9.6	50	100	400
$^4S_{3/2} - ^2D_{3/2}$	2.60	4.89-1	2.46-1	6.18-2
$^4S_{3/2} - ^2D_{5/2}$	8.22	1.50	7.50-1	1.88-1
$^4S_{3/2} - ^2P_{1/2}$	4.69-1	8.59-2	4.29-2	1.07-2
$^4S_{3/2} - ^2P_{3/2}$	2.04-2	3.26-3	1.55-3	3.79-4
$^2D_{3/2} - ^2D_{5/2}$	5.36	1.05	5.27-1	1.32-1
$^2D_{3/2} - ^2P_{1/2}$	1.11+1	2.18	1.10	2.78-1
$^2D_{3/2} - ^2P_{3/2}$	6.87	1.28	6.44-1	1.62-1
$^2D_{5/2} - ^2P_{1/2}$	6.18	1.16	5.75-1	1.43-1
$^2D_{5/2} - ^2P_{3/2}$	1.08+1	2.00	1.01	2.57-1
$^2P_{1/2} - ^2P_{3/2}$	6.26	1.25	6.28-1	1.58-1

Table 2: The proton excitation total rate constants , $\alpha(10^{-10}$ cm^{2}s$^{-1})$. Here $a \pm b \equiv a \times 10^{\pm b}$.

T, 10^6 K	3	6	9	12	15
$^4S_{3/2} - ^2D_{3/2}$	7.12-3	5.83-2	1.28-1	1.91-1	2.41-1
$^4S_{3/2} - ^2D_{5/2}$	1.21-2	1.23-1	3.03-1	4.78-1	6.25-1
$^4S_{3/2} - ^2P_{1/2}$	3.42-4	4.21-3	1.13-2	1.94-2	2.63-2
$^4S_{3/2} - ^2P_{3/2}$	1.09-5	1.33-4	3.86-4	6.84-4	9.72-4
$^2D_{3/2} - ^2D_{5/2}$	1.31-1	3.38-1	5.25-1	6.56-1	7.43-1
$^2D_{3/2} - ^2P_{1/2}$	1.10-1	4.42-1	8.06-1	1.11	1.35
$^2D_{3/2} - ^2P_{3/2}$	9.77-3	1.03-1	2.52-1	3.96-1	5.17-1
$^2D_{5/2} - ^2P_{1/2}$	8.31-2	3.21-1	6.31-1	8.97-1	1.10
$^2D_{5/2} - ^2P_{3/2}$	8.34-2	3.69-1	7.64-1	1.09	1.34
$^2P_{1/2} - ^2P_{3/2}$	1.46-1	3.48-1	5.58-1	7.14-1	8.23-1
T, 10^6 K	30	60	120	240	600
$^4S_{3/2} - ^2D_{3/2}$	3.51-1	3.66-1	3.18-1	2.48-1	1.73-1
$^4S_{3/2} - ^2D_{5/2}$	9.94-1	1.06	8.87-1	6.75-1	4.27-1
$^4S_{3/2} - ^2P_{1/2}$	4.62-2	5.24-2	4.21-2	3.22-2	2.21-2
$^4S_{3/2} - ^2P_{3/2}$	1.89-3	2.12-3	1.58-3	1.11-3	8.10-4
$^2D_{3/2} - ^2D_{5/2}$	8.84-1	8.19-1	6.57-1	4.95-1	3.08-1
$^2D_{3/2} - ^2P_{1/2}$	1.86	1.93	1.68	1.32	8.55-1
$^2D_{3/2} - ^2P_{3/2}$	8.19-1	8.83-1	7.53-1	5.82-1	3.68-1
$^2D_{5/2} - ^2P_{1/2}$	1.53	1.59	1.40	1.12	8.45-1
$^2D_{5/2} - ^2P_{3/2}$	1.79	1.76	1.49	1.15	9.35-1
$^2P_{1/2} - ^2P_{3/2}$	1.00	9.56-1	7.98-1	6.16-1	4.22-1

temperatures. One M_J component of the initial state and all the $M_{J'}$ components, up to six, were included into the close coupling model. Our results show that the only available semiclassical results (the first perturbative approximation of the impact parametre approach with the Coulomb trajectories of the nuclei) [6] may in many cases overestimate the rate constants with a factor reaching two. To make the final conclusion we plan to recompute all the cross sections and the rate constants using the enlarged close coupling scheme. It seems also desirable to take into account the deviation of the "exact" trajectory of proton from the Coulomb hyperbola and the change of the proton speed during the collision. The inclusion of the interaction with the nearest levels of the higher configuration, at least in the model of the polarization potential, may also influence the final resuls.

Acknowledgements

We thank Professor H. Tawara for useful references and Professor V. P. Shevelko (Lebedev Physical Institute, Russia, visiting NIFS) for help in computing Born-Coulomb excitation cross sections with ATOM program. One of us (A. D. Ulantsev) thanks Professor K. Sato and Doctor D. Kato for help in organizing his visit to NIFS.

Appendix

A Wave functions and matrix elements of the interaction.

Semiempirical one-electron basis functions (orbitals) were computed using the ATOM program [9]. The program computes radial one-electron functions as eigenfunctions of the radial Schrödinger equation with the spherically symmetric potential taking into account contributions of all the occupied states described by nodeless Slater orbitals. The solution in question is forced to have the necessary number of nodes. If the eigenenergy of the one-electron state in question is known from more elaborate computations or from the analysis of the data, the potential is scaled so that the eigenfunction corresponds to this eigenenergy. In the opposite case both the eigenfunction and eigenenergy are defined together. Though the ATOM program allows to include the exchange potential into the radial Schrödinger equation for the one-electron functions, we did not include the exchange as its effect is negligible on this step. Wave functions of different states of the p^3 configuration in the LS coupling scheme may be expressed explicitly as linear combinations of Slater determinants. We obtained the wave function component with $M_S = 3/2$ of the zero-order ^4S ($S = 3/2$, $L = 0$) state by means of one determinant (see for example [10], ch. 5 and [14]) that in standard notations of Condon and Shortley [15] has the form

$$\Psi(S = \frac{3}{2}, L = 0, M_S = \frac{3}{2}, M_L = 0) = |1^+, 0^+, -1^+| \qquad \text{(A1)}$$

We recall that here the numbers designate orbital magnetic numbers m_l for individual electrons, and signs in the superscript designate the signs of spin magnetic numbers m_s for individual electrons. The normalizing factor $1/\sqrt{3!}$ is supposed to be included into the expressions. Next the wave functions ^4S with smaller M_S were obtained using the lowering operator for the spin projection $\hat{S}^-$ [10]

$$\hat{S}^- = \sum_{k=1}^{3} \hat{s}_k^- = \sum_{k=1}^{3} (\hat{s}_{k,x} - i\hat{s}_{k,y}) \tag{A2}$$

Correspondingly

$$\Psi(S = \frac{3}{2}, L = 0, M_S = \frac{1}{2}, M_L = 0) = \frac{1}{\sqrt{3}}(|1^-, 0^+, -1^+| + |1^+, 0^-, -1^+| + |1^+, 0^+, -1^-|) \tag{A3}$$

The wave function of the zero-order ^2D ($S = 1/2$, $L = 2$) state with the $M_L = 2$ component is also expressed as one determinant

$$\Psi(S = \frac{1}{2}, L = 2, M_S = \frac{1}{2}, M_L = 2) = |1^+, 1^-, 0^+| \tag{A4}$$

The components ^2D with lower values of M_L are obtained using the orbital momentum lowering operator $\hat{L}^-$ [10]

$$\hat{L}^- = \sum_{k=1}^{3} \hat{l}_k^- = \sum_{k=1}^{3} (\hat{l}_{k,x} - i\hat{l}_{k,y}) \tag{A5}$$

Then

$$\Psi(S = \frac{1}{2}, L = 2, M_S = \frac{1}{2}, M_L = 1) = \frac{1}{\sqrt{2}}(|1^+, 1^-, -1^+| - |1^+, 0^+, 0^-|) \tag{A6}$$

and

$$\Psi(S = \frac{1}{2}, L = 2, M_S = \frac{1}{2}, M_L = 0) = \frac{1}{\sqrt{6}}(|1^+, 0^+, -1^-| - 2|1^+, 0^-, -1^+| + |1^-, 0^+, -1^+|) \tag{A7}$$

The wave function for ^2P state with $M_L = 1$ and $M_S = 1/2$ may be constructed from the same two determinants that form the ^2D with the same M_L and M_S if we use the orthogonality condition

$$<^2 P, M_S = \frac{1}{2}, M_L = 1|^2 D, M_S = \frac{1}{2}, M_L = 1 >= 0 \tag{A8}$$

Then

$$\Psi(S = \frac{1}{2}, L = 1, M_S = \frac{1}{2}, M_L = 1) = \frac{1}{\sqrt{2}}(|1^+, 1^-, -1^+| + |1^+, 0^+, 0^-|) \tag{A9}$$

And then using the the orbital momentum lowering operator $\hat{L}^-$ from eq. (A5)

$$\Psi(S = \frac{1}{2}, L = 1, M_S = \frac{1}{2}, M_L = 0) = \frac{1}{\sqrt{2}}(|1^+, 0^+, -1^-| - |1^-, 0^+, -1^+|) \tag{A10}$$

The wave functions of the components with the negative signs of M_L and M_S are obtained from the corresponding expressions (A1) – (A10) by the change of the signs of all the m_l or/and m_l for the spin-orbitals in the determinants. The wave functions with definite J and M_J are expressed as linear combinations of the corresponding wave functions with definite M_L and M_S

$$\Psi_{L,S,J,M_J} = \sum_{M_L,M_S} (LM_LSM_S|JM_J)\Psi_{L,S,M_L,M_S} \tag{A11}$$

where $(LM_LSM_S|JM_J)$ are the corresponding Clebsch-Gordan coefficients [10, 16]. The Clebsch-Gordan coefficients, or strictly saying Wigner $3j$ symbols differenting from the Clebsch-Gordan coefficients only with simple factors, are tabulated for almost any practical case in [16]. The program for the computation of $3j$ symbols is available free in the Internet [18]. It is worth noting that Ψ_{L,S,J,M_J} so constructed are in fact wave functions of zero approximation in a sense that they take into account only effects of the static central averaged potential $V_{res}(r)$ (see details in [9]). Taking into account both the direct electron-electron pair interaction $U_{ee}(\mathbf{r}_j,\mathbf{r}_k) = 1/|\mathbf{r}_j - \mathbf{r}_k|$ and the main relativistic corrections, that is the spin-orbit and spin-spin ineractions, we obtain the system of equations for coefficients of the matrix connecting the intermediate coupling wave functions $\varphi(^{2S+1}L', J, M_J) = \Psi(^{2S+1}L'_{J,M_J})$ for the physical states with the wave functions of LS zero approximation $\Psi(^{2S+1}L_{J,M_J}) = \Psi_{L,S,J,M_J}$ [16, 17]

$$\begin{aligned}
\Psi(^4S'_{3/2,M_J}) &= a_S\Psi(^4S_{3/2,M_J}) + b_S\Psi(^2D_{3/2,M_J}) + c_S\Psi(^2P_{3/2,M_J})\\
\Psi(^2D'_{3/2,M_J}) &= a_D\Psi(^4S_{3/2,M_J}) + b_D\Psi(^2D_{3/2,M_J}) + c_D\Psi(^2P_{3/2,M_J})\\
\Psi(^2P'_{3/2,M_J}) &= a_P\Psi(^4S_{3/2,M_J}) + b_P\Psi(^2D_{3/2,M_J}) + c_P\Psi(^2P_{3/2,M_J})\\
\Psi(^2D'_{5/2,M_J}) &= \Psi(^2D_{5/2,M_J})\\
\Psi(^2P'_{1/2,M_J}) &= \Psi(^2P_{1/2,M_J})
\end{aligned} \tag{A12}$$

The coefficients a_L, b_L, c_L may be defined simultaneously with the corrected energies $E(^{2S+1}L_J$ from the secular equation that for $J = \frac{3}{2}$ has the form [14]

$$\begin{aligned}
&\left(E_0(^2D) + \frac{111}{10}\eta\right)a + \frac{1}{2}\zeta\sqrt{5}b - \frac{6\zeta}{\sqrt{5}}c = Ea\\
&\frac{1}{2}\zeta\sqrt{5}a + \left(E_0(^2P) - \frac{5\zeta}{2}\right)b + \zeta c = Eb\\
&-\frac{6\zeta}{\sqrt{5}}a + \zeta b + E_0(^4S)c = Ec
\end{aligned} \tag{A13}$$

For the remaining levels $J = \frac{5}{2}$ and $J = \frac{1}{2}$ the energy corrections have the forms [14]

$$\begin{aligned}
E(^2D_{5/2}) &= E_0(^2D) - \frac{37\eta}{5}\\
E(^2P_{1/2}) &= E_0(^2P) + 5\eta
\end{aligned} \tag{A14}$$

where ζ and η indicate one-electron matrix elements of the spin-orbit and spin-spin interaction respectively . The explicit expression for η and ζ have the forms [14]

$$\eta = \frac{1}{4c^2}\int_0^\infty\int_0^{r_2} r_2^{-3}R^2_{2p}(r_1)R^2_{2p}(r_2)dr_1dr_2 \tag{A15}$$

$$\zeta = \frac{1}{2c^2}\int_0^\infty r^{-1}(-\frac{dV_{res}(r)}{dr})R_{2p}^2(r)dr \qquad \text{(A16)}$$

It is important to notice that in equations (A12, A14) the initial LS energies $E_0(^{2S+1}L)$ include the contributions from the direct electron-electron interactions $U_{ee}(\mathbf{r}_j, \mathbf{r}_k)$.

The numerical solutions of the equations (A13, A14) for the case in question were published in [17] (there it was supposed $\eta = 0$). The results of [17] that we used are

$$\begin{aligned} &a_S = 0.9279, \quad b_S = +0.1709, \quad c_S = -0.3314, \\ &a_D = -0.3003, \quad b_D = +0.8694, \quad c_D = -0.3924, \\ &a_P = 0.2211, \quad b_P = +0.4636, \quad c_P = 0.8580. \end{aligned} \qquad \text{(A17)}$$

Taking into account the fact that the energies $E(^{2S+1}L_J)$ were calculated earlier with high accuracy using substantially more elaborate approach including the configuration interaction of many states [19] it might be practical to use in future just these energies as initial data and to compute $E_0(^2L)$, ζ and η as auxiliary parametres.

Using the eq. (A11) one may express matrix elements of the electrostatic potential of the projectile $V(\mathbf{r}_1, ...\mathbf{r}_3; \mathbf{R}(t))$, eq. (3) as

$$\begin{aligned} &< \Psi_{L,S,J,M_J}|V(\mathbf{r}_1, ...\mathbf{r}_3; \mathbf{R}(t))|\Psi_{L',S',J',M'_J} >= \\ &\sum_{M_L,M_S}\sum_{M'_L,M'_S}(LM_LSM_S|JM_J)(L'M'_LS'M'_S|JM_J) \\ &\times < \Psi_{L,S,M_L,M_S}|V(\mathbf{r}_1, ...\mathbf{r}_3; \mathbf{R}(t))|\Psi_{L',S',M'_L,M'_S} > . \end{aligned} \qquad \text{(A18)}$$

The direct calculation of the matrix elements (A18) with the wave functions (A1-A10) gives the expressions in terms of the matrix elements of the one-electron interaction operator $u(\mathbf{r}) = Z_P/|\mathbf{r} - \mathbf{R}|$ over one-electron wave functions $\chi_{2p,m}(\mathbf{r}) \equiv |m >$. The necessary expressions are given in the table 3.

The remaining non-zero matrix elements are

$$\begin{aligned} &< \Psi(^4S, M_S = \frac{3}{2})|V(\mathbf{r}_1, ...\mathbf{r}_3; \mathbf{R}(t))|\Psi(^4S, M_S = \frac{3}{2}) >= \\ &< \Psi(^4S, M_S = \frac{1}{2})|V(\mathbf{r}_1, ...\mathbf{r}_3; \mathbf{R}(t))|\Psi(^4S, M_S = \frac{1}{2}) >= \\ &< 1|u|1 > + < 0|u|0 > + < -1|u| - 1 > \end{aligned} \qquad \text{(A19)}$$

The one electron matrix elements $< m|u|m' >$ were calculated numerically after the separation of the angular parts according to the standard schemes [16, 9].

Table 3: The matrix elements V_{jk}^{LS} for the LS states with $S = \frac{1}{2}, \quad M_S = \frac{1}{2}$

	$P, M_L = 1$
$D, M_L = 2$	$\frac{1}{\sqrt{2}}(<0\|u\|-1> - <1\|u\|0>)$
$D, M_L = 1$	$\frac{1}{2}(<1\|u\|1> -2<0\|u\|0> +2<-1\|u\|-1>)$
$D, M_L = 0$	$\frac{\sqrt{3}}{2}(<0\|u\|1> - <-1\|u\|0>)$
$P, M_L = 1$	$\frac{1}{\sqrt{2}}(3<1\|u\|1> +2<0\|u\|0> + <-1\|u\|-1>)$
$P, M_L = 0$	$\frac{1}{2}(<-1\|u\|0> + <0\|u\|1>)$

	$P, M_L = 0$	$P, M_L = -1$
$D, M_L = 2$	$-\sqrt{2}<1\|u\|-1>$	0
$D, M_L = 1$	$\frac{1}{2}(<1\|u\|0> - <0\|u\|-1>)$	$- <1\|u\|-1>$
$D, M_L = 0$	0	$\frac{\sqrt{3}}{2}(1\|u\|0> - <0\|u\|-1>)$
$P, M_L = 1$	$\frac{1}{2}(<0\|u\|-1> + <1\|u\|0>)$	0
$P, M_L = 0$	$<1\|u\|1> + <0\|u\|0> + <-1\|u\|-1>$	$\frac{1}{2}(<1\|u\|0> + <0\|u\|-1>)$

	$D, M_L = 2$
$D, M_L = 2$	$2<1\|u\|1> + <0\|u\|0>$
$D, M_L = 1$	$\frac{1}{\sqrt{2}}(<1\|u\|0> + <0\|u\|-1>$
$D, M_L = 0$	0

	$D, M_L = 1$
$D, M_L = 2$	$\frac{1}{\sqrt{2}}(<1\|u\|0> + <0\|u\|-1>$
$D, M_L = 1$	$\frac{1}{2}(3<1\|u\|1> +2<0\|u\|0> + <-1\|u\|-1>)$
$D, M_L = 0$	$\frac{\sqrt{3}}{2}(<1\|u\|0> + <0\|u\|-1>$

	$D, M_L = 0$
$D, M_L = 2$	0
$D, M_L = 1$	$\frac{\sqrt{3}}{2}(<1\|u\|0> + <0\|u\|-1>$
$D, M_L = 0$	$<1\|u\|1> + <0\|u\|0> + <-1\|u\|-1>$

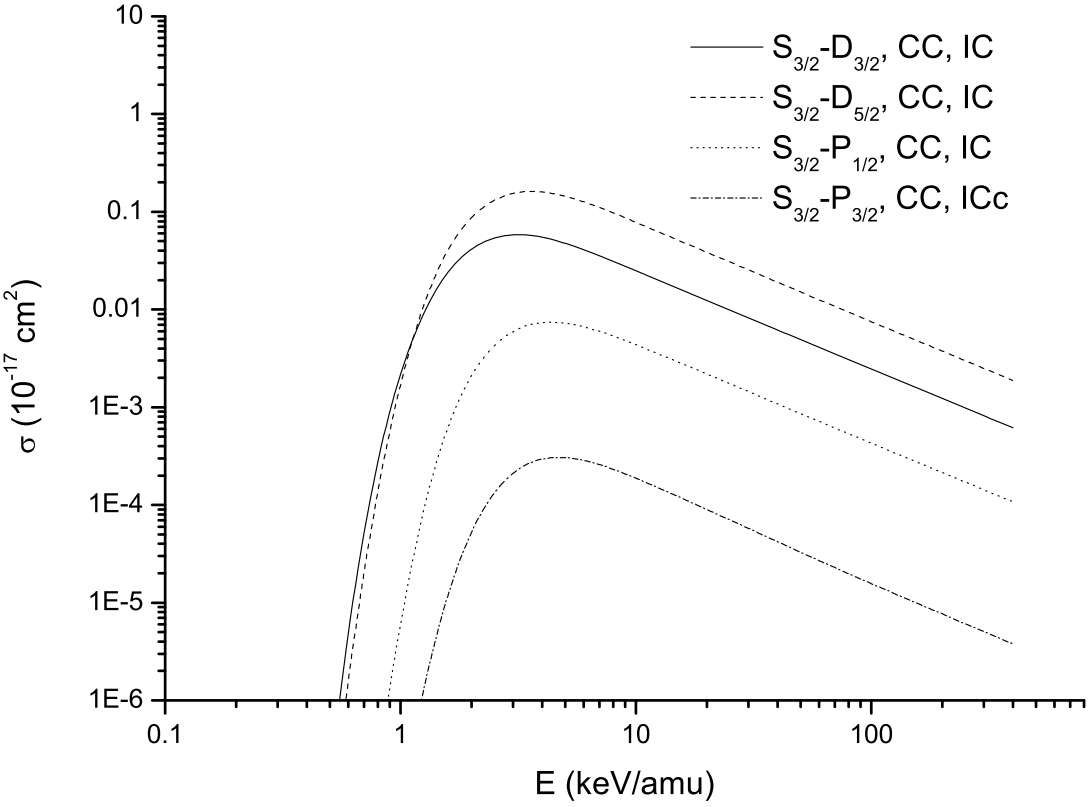

Figure 1: The proton excitation total cross sections for the ${}^4S_{3/2} - {}^2L_J$ transitions. CC (close-coupling): ${}^4S_{3/2} - {}^2D_{3/2}$ solid line, ${}^4S_{3/2} - {}^2D_{5/2}$ dash line , ${}^4S_{3/2} - {}^2P_{1/2}$ dot line, ${}^4S_{3/2} - {}^2P_{3/2}$ dash dot line.

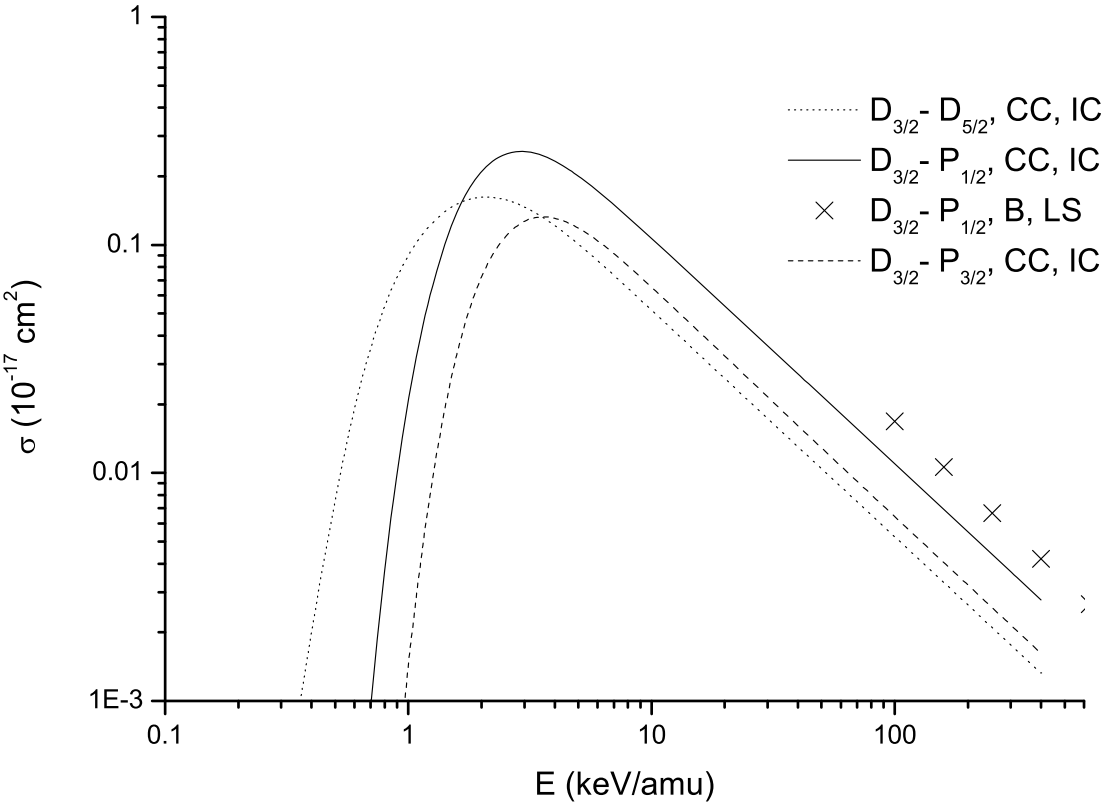

Figure 2: The proton excitation total cross sections for the ${}^2D_{3/2} - {}^2L_J$ transitions. CC (close-coupling): ${}^2D_{3/2} - {}^2D_{5/2}$ dot line, ${}^2D_{3/2} - {}^2P_{1/2}$ solid line, ${}^2D_{3/2} - {}^2P_{3/2}$ dash line; B (Born-Coulomb): ${}^2D_{3/2} - {}^2P_{1/2}$ crosses.

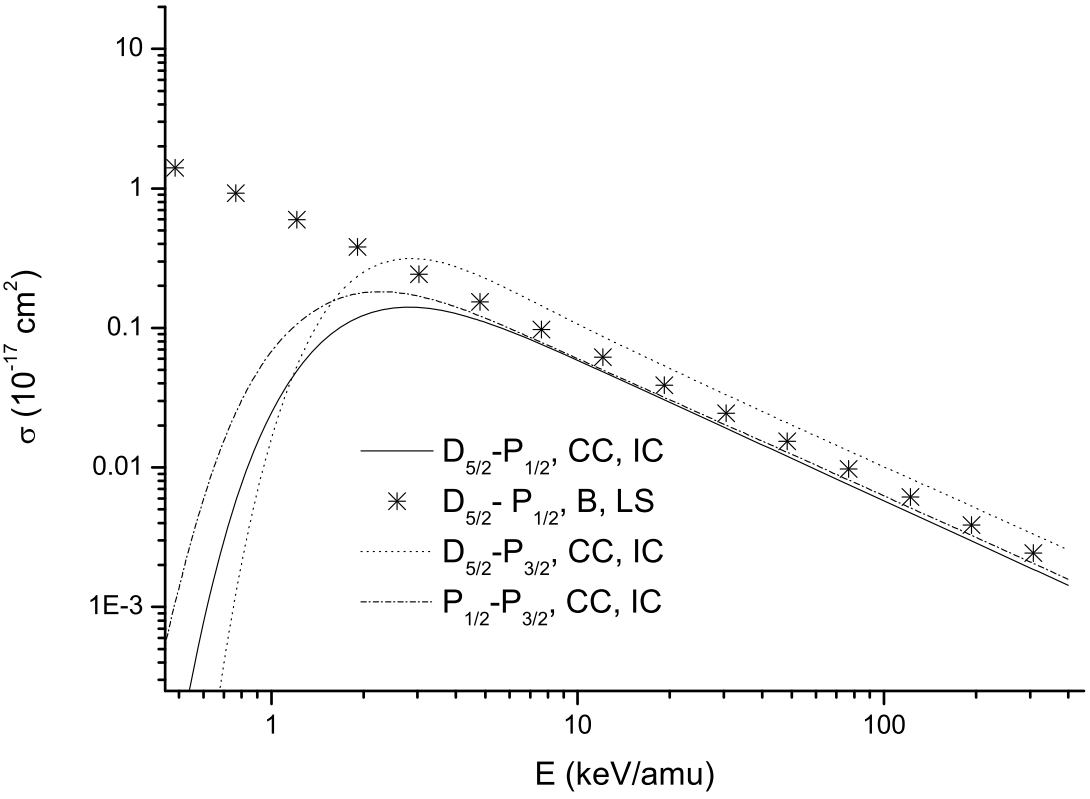

Figure 3: The proton excitation total cross sections for the ${}^2D_{5/2} - {}^2L_J$ and ${}^2P_{1/2} - {}^2P_{3/2}$ transitions. CC (close-coupling): ${}^2D_{5/2} - {}^2P_{1/2}$ solid line, ${}^2D_{5/2} - {}^2P_{3/2}$ dash line, ${}^2P_{1/2} - {}^2P_{3/2}$ dot line; B (Born-Coulomb): ${}^2D_{5/2} - {}^2P_{1/2}$ crosses.

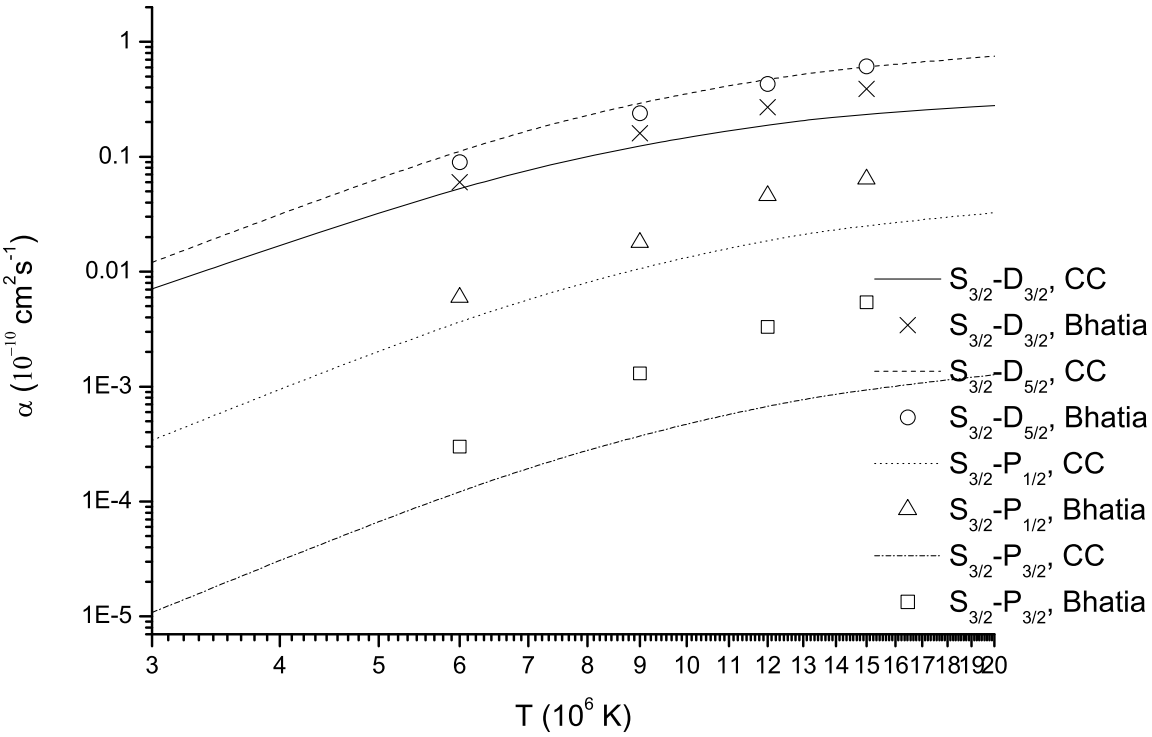

Figure 4: The proton excitation rate constants for the ${}^4S_{3/2} - {}^2L_J$ transitions. CC (close coupling): ${}^4S_{3/2} - {}^2D_{3/2}$ solid line, ${}^4S_{3/2} - {}^2D_{5/2}$ dash line, ${}^4S_{3/2} - {}^2P_{1/2}$ dot line, ${}^4S_{3/2} - {}^2P_{3/2}$ dash dot line; Bhatia [6], SC: ${}^4S_{3/2} - {}^2D_{3/2}$ crosses, ${}^4S_{3/2} - {}^2D_{5/2}$ circles, ${}^4S_{3/2} - {}^2P_{1/2}$ triangles, ${}^4S_{3/2} - {}^2P_{3/2}$ squares.

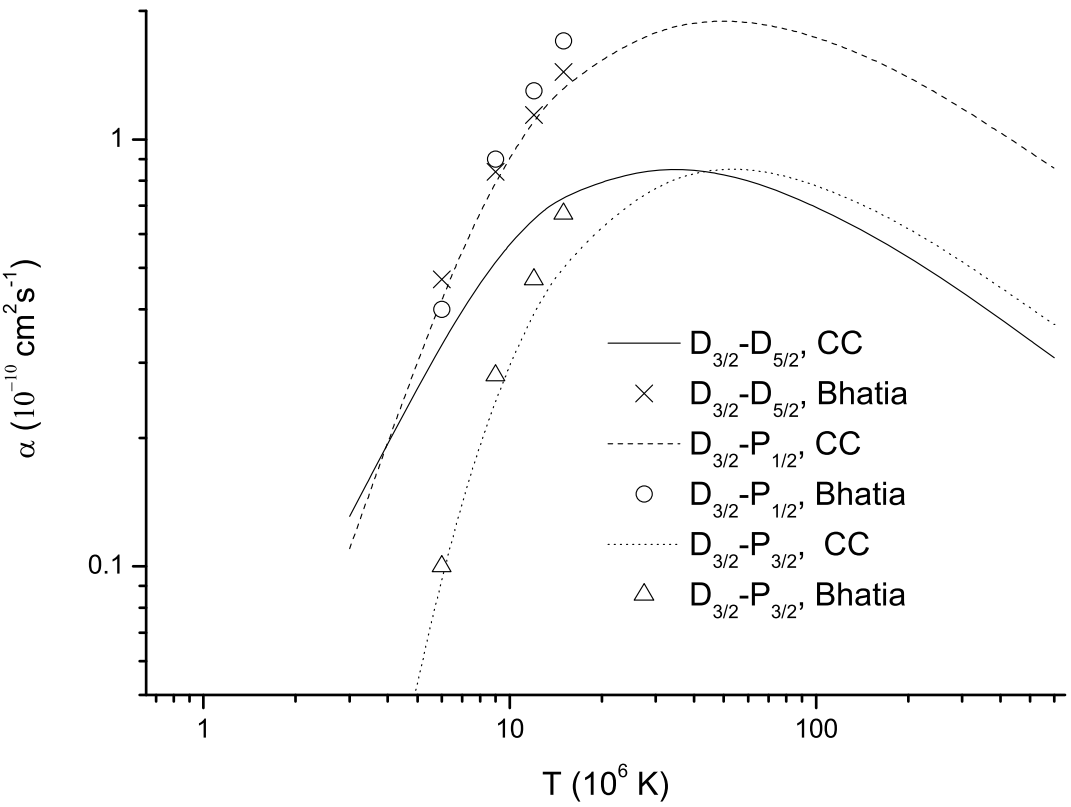

Figure 5: The proton excitation rate constants for the ${}^2D_{3/2} - {}^2 L_J$ transitions. CC (close coupling): ${}^2D_{3/2} - {}^2 D_{5/2}$ solid line, ${}^2D_{3/2} - {}^2 P_{1/2}$ dash line, ${}^2D_{3/2} - {}^2 P_{3/2}$ dot line; Bhatia [6], SC: ${}^2D_{3/2} - {}^2 D_{5/2}$ crosses, ${}^2D_{3/2} - {}^2 P_{1/2}$ circles, ${}^2D_{3/2} - {}^2 P_{3/2}$ triangles.

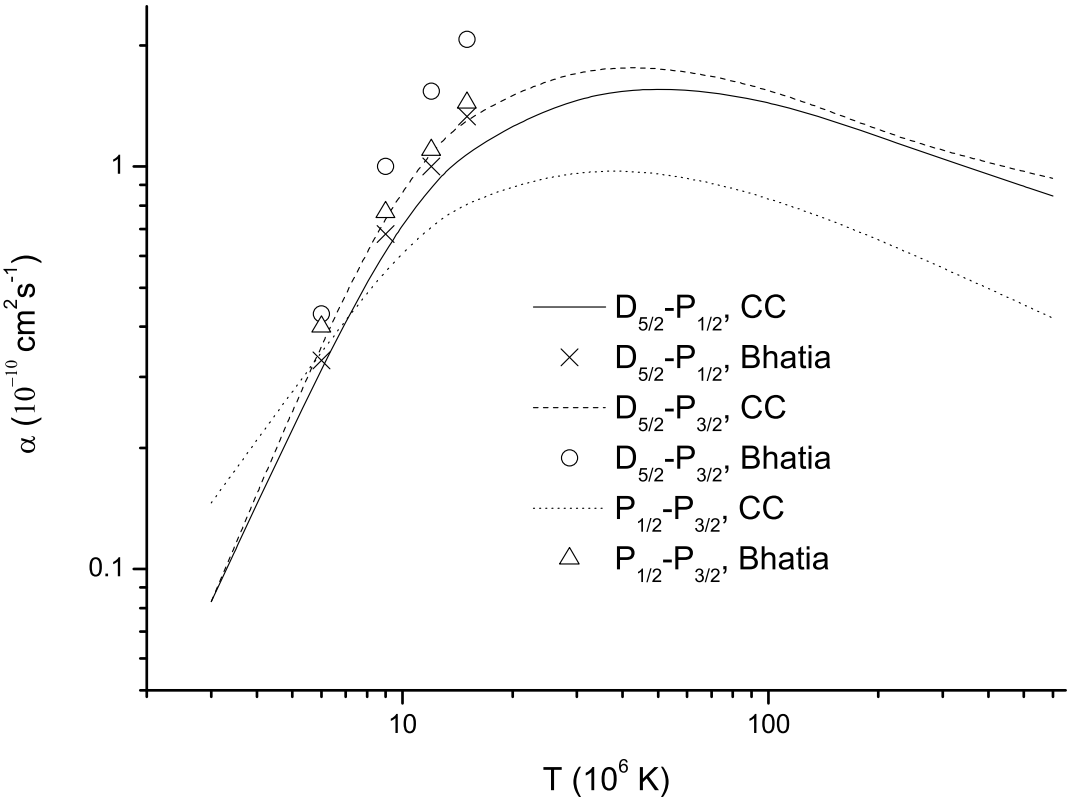

Figure 6: The proton excitation rate constants for the ${}^2D_{5/2} - {}^2L_J$ and ${}^2P_{1/2} - {}^2P_{3/2}$ transitions. CC (close coupling): ${}^2D_{5/2} - {}^2P_{1/2}$ solid line, ${}^2D_{5/2} - {}^2P_{3/2}$ dash line, ${}^2P_{1/2} - {}^2P_{3/2}$ dot line; Bhatia [6], SC: ${}^2D_{5/2} - {}^2P_{1/2}$ crosses, ${}^2D_{5/2} - {}^2P_{3/2}$ circles, ${}^2P_{1/2} - {}^2P_{3/2}$ triangles.

References

[1] Seaton, M. J. (1964) *Month. Not. R. Astr. Soc.*, **127**, 91.

[2] Walling, R. S. and Weisheit, J. C. (1988) *Phys. Rep*, **162**, 1.

[3] Skobelev, I., Murakami, I. and Kato, T. (2007) *NIFS-DATA-099.*

[4] Skobelev, I., Murakami, I. and Kato, T. (2006) *NIFS-DATA-095.*

[5] Skobeoev, I., Murakami, I. and Kato, T. (2010) *Astron. Astrophys.*, **511**, A60.

[6] Bhatia, A. K. and Mason, H. E. (1980) *Astron. Astrophys.*, **83**, 380.

[7] Alder, K., Bohr, A., Huus, T., Mottleson, B. and Winther, A. (1956) *Rev. Mod. Phys.*, **28**, 432.

[8] Reid, R. H. G. (1988) *Advan. Atom. Molec. Phys.*, **25**, 251.

[9] Shevelko, V. P. and Vainshtein, L. A. (1993) *Atomic Physics for Hot Plasmas*, Bristol: IOP Publ.

[10] Landau, L. D. and Lifshitz, E.M. (2003) *Quantum Mechanics: The Nonrelativistic Theory*, Elsevier Science Ltd.

[11] Foster, V. J., Keenan, F. P. and Reid, R. H. G (1979) *At. Data Nucl. Data Tables*, **67**, 99.

[12] Heil, T. G., Green, S. and Dalgarno, A. (1982) *Phys. Rev. A*, **26**, 3293.

[13] Heil, T. G., Kirby, K. and Dalgarno, A. (1983) *Phys. Rev. A*, **27**, 2826.

[14] Aller, L. H., Ufford, C. W. and Van Vleck, J. H. (1949) *Astrophys. J.*, **109**, 42.

[15] Condon, E. U. and Shortley, G. H. (1991) *The Theory of Atomic Spectra*, Cambridge: the University Press.

[16] Sobelman, I. I. (1992) *Atomic Spectra and Radiative Transitions*, 2nd ed., Springer-Verlag.

[17] Curtis, L. J. (2003) *Atomic Structure and Lifetimes: A Conceptual Approach*, Cambridge: University Press.

[18] Stone, A., http://www-stone.ch.cam.ac.uk/wigner.shtml

[19] Cheng, K. T., Kim, Y. K. and Desclaux, J. P. (1979) *At. Data Nucl. Data Tables*, **24**, 111.